

# Suppression of KIF2 in PC12 Cells Alters the Distribution of a Growth Cone Nonsynaptic Membrane Receptor and Inhibits Neurite Extension

Gerardo Morfini,\* Santiago Quiroga,‡ Alberto Rosa,‡ Kenneth Kosik,§ and Alfredo Cáceres\*

\*Instituto Investigación Médica Mercedes y Martín Ferreyra, 5000 Córdoba, Argentina; ‡Departamento Química Biológica, Facultad Ciencias Químicas (CIQUIBIC) Universidad Nacional de Córdoba/CONICET, 5000 Córdoba, Argentina; and §Department of Neurology (Neuroscience), Harvard Medical School and Center for Neurological Diseases, Department of Medicine (Division of Neurology), Brigham and Women's Hospital, Boston, Massachusetts 02115

**Abstract.** In the present study, we present evidence about the cellular functions of KIF2, a kinesin-like superfamily member having a unique structure in that its motor domain is localized at the center of the molecule (Noda Y., Y. Sato-Yoshitake, S. Kondo, M. Nangaku, and N. Hirokawa. 1995. *J. Cell Biol.* 129:157–167.). Using subcellular fractionation techniques, isopicnic sucrose density centrifugation of microsomal fractions from developing rat cerebral cortex, and immunoisolation with KIF2 antibodies, we have now identified a type of nonsynaptic vesicle that associates with KIF2. This type of organelle lacks synaptic vesicle markers (synapsin, synaptophysin), amyloid precursor protein, GAP-43, or N-cadherin. On the other hand, it contains  $\beta_{gc}$ , which is a novel variant of the  $\beta$  subunit of the IGF-1 receptor, which is highly enriched in growth cone membranes. Both  $\beta_{gc}$  and KIF2 are upregulated by NGF in PC12 cells and highly concentrated in growth cones of developing neurons. We have also analyzed the conse-

quences of KIF2 suppression by antisense oligonucleotide treatment on nerve cell morphogenesis and the distribution of synaptic and nonsynaptic vesicle markers. KIF2 suppression results in a dramatic accumulation of  $\beta_{gc}$  within the cell body and in its complete disappearance from growth cones; no alterations in the distribution of synapsin, synaptophysin, GAP-43, or amyloid precursor protein are detected in KIF2-suppressed neurons. Instead, all of them remained highly enriched at nerve terminals. KIF2 suppression also produces a dramatic inhibition of neurite outgrowth; this phenomenon occurs after  $\beta_{gc}$  has disappeared from growth cones. Taken collectively, our results suggest an important role for KIF2 in neurite extension, a phenomenon that may be related with the anterograde transport of a type of nonsynaptic vesicle that contains as one of its components a growth cone membrane receptor for IGF-1, a growth factor implicated in nerve cell development.

**D**URING recent years it has become increasingly evident that the assembly of the neuronal cytoskeleton and the transport of membrane precursors to the active growing tip of neuritic processes are the two basic events underlying process formation in developing neurons (Mitchison and Kirschner, 1988; Tanaka and Sabry, 1995). Because axons and their growth cones lack protein synthetic machinery, highly specialized intracellular transport mechanisms must exist to deliver appropriate cargoes to their final destinations and/or to sites of membrane addition.

The microtubule-based anterograde fast axonal transport is one of the mechanisms by which tubulovesicular structures, synaptic membrane precursors, and nonsynap-

tic membrane-bound organelles are distributed along axonal processes (Hirokawa, 1996). Kinesin, the first discovered and characterized anterograde microtubule-based motor (Brady, 1985; Scholey et al., 1985; Vale et al., 1985a), has been involved in the transport of tubulovesicular organelles such as the endoplasmic reticulum (Feiguin et al., 1994), endosomes and lysosomes (Hollenbeck and Swanson, 1990; Feiguin et al., 1994; Nakata and Hirokawa, 1995), as well as of certain groups of vesicles containing GAP-43, synapsin I, and amyloid precursor protein (Ferreira et al., 1992, 1993). However, recent studies have provided evidence indicating that kinesin is not the only anterograde microtubule-based motor involved in organelle transport within axons. Thus, molecular genetic approaches have identified a series of gene-encoding proteins sharing a domain of 350 amino acids, which contains a putative ATP-binding site and a microtubule-binding domain homologous to that of kinesin heavy chain (for reviews see

Please address all correspondence to Alfredo Cáceres, Instituto Mercedes y Martín Ferreyra, Casilla de Correo 389, 5000 Córdoba, Argentina. Tel.: 54-51-681465. FAX: 54-51-95163. e-mail: acaceres@immf.uncor.edu

Endow, 1991; Goldstein, 1991; Hirokawa, 1993, 1996). In the particular case of murine brain tissue, a systematic search for novel putative motors led to the initial discovery of 11 members of the kinesin superfamily (Aizawa et al., 1992; Kondon et al., 1994; Okada et al., 1995; Noda et al., 1995; Yamazaki et al., 1995; Hirokawa, 1996). More importantly, the function of at least some of these proteins has already been established. For example, KIF1A, the murine homologue of unc104 kinesin (Hall and Hedgecock, 1991), is a monomeric motor involved in the anterograde transport of synaptic vesicle precursors (Okada et al., 1995), while mitochondria are conveyed anterogradely by KIF1B (Nangaku et al., 1994).

KIF2 is one kinesin superfamily member having a unique structure in that its motor domain is localized at the center of the molecule (Aizawa et al., 1992; Noda et al., 1995). There is considerable interest in defining KIF2 function since this molecule may have an important role in the transport of membranous organelles to the active growing tip of axonal processes. Thus, KIF2 is predominantly expressed in developing brain tissue, where it is highly enriched in growth cones and appears to be specialized for the transport of membranous organelles different from those carried by kinesin heavy chain (KHC),<sup>1</sup> KIF1A (Okada et al., 1995), KIF1B (Nangaku et al., 1994), or KIF3A/B (Noda et al., 1995).

With these considerations in mind, in the present study we examined the cellular functions of KIF2 in mammalian neurons. To approach this problem, subcellular fractionation techniques and immunoisolation experiments of membrane organelles with antibodies against KIF2 were initially used to obtain some insight about the nature of the cargo that KIF2 may transport. We then analyzed the pattern of expression, subcellular localization, and consequences of KIF2 suppression by antisense oligonucleotide treatment on the distribution of several growth cone membrane proteins and neurite outgrowth in PC12 cells. Taken collectively, the results obtained suggest an important role for KIF2 in neurite extension, a phenomenon that may be related with the anterograde transport of a type of nonsynaptic vesicle that contains as one of its components a growth cone membrane protein designated  $\beta_{gc}$ , which is a novel variant of the  $\beta$  subunit of the IGF-1 receptor (Quiroga et al., 1995; Mascotti et al., 1997).

## Materials and Methods

### Cultures

The rat pheochromocytoma cell line (PC12 cells) was obtained from Dr. Adriana Ferreira (Center Neurological Diseases, Harvard Medical School, Boston, MA). They were grown on DME supplemented with 10% horse serum. Cells were plated onto polylysine-treated glass coverslips (Mascotti et al., 1997) at densities ranging from 5,000–20,000 cells/cm<sup>2</sup>. 2 d after plating, the coverslips with the attached cells were transferred to Petri dishes containing serum-free medium supplemented with the N<sub>2</sub> mixture of Bottenstein and Sato (1979). To induce the differentiation of PC12 cells, NGF (Boehringer Mannheim Chemicals, Indianapolis, IN) was added to the culture medium at a concentration of 50 ng/ml.

1. *Abbreviations used in this paper:* APP, amyloid precursor protein; KHC, kinesin heavy chain; PVDF, polyvinylidene difluoride; SV, synaptic vesicle.

### Antisense Oligonucleotides

Antisense phosphorothioate oligonucleotides (S-modified) were used in the present study. The initial experiments were performed with oligonucleotides  $-11/+14$  of the sequence of mouse KIF2 (Aizawa et al., 1992; Noda et al., 1995). However, because, PC12 cells are of rat origin, these experiments were subsequently repeated using oligonucleotides corresponding to the rat KIF2 sequence. The rat sequence in the region of the KIF2 motor domain was obtained by using nondegenerate, 18-mer mouse primers, and performing PCR on reverse-transcribed rat brain mRNA. An amplified band of the expected size was obtained and the DNA was cloned and sequenced. Analysis of the obtained sequence revealed >96% homology with the reported sequence of mouse KIF2 (Noda et al., 1995). One of the oligonucleotides designated ASKF2a corresponds to the sequence ACATGTCATGGCTCCGAGATG, and is the inverse complement of nucleotides +830/851 of the sequence of the motor domain of rat KIF2; antisense oligonucleotide ASKF2b, consisting of the sequence CACTGTCATGGCTCCG, is the inverse complement of the rat nucleotides +831/845. Both of the regions selected from the sequence of the rat KIF2 motor domain are identical to the corresponding regions in the mouse KIF2 sequence.

The oligonucleotides were purchased from Quality Controlled Biochemicals (Hopkinton, MA); they were purified by reverse chromatography, and taken up in serum-free medium as described previously (Cáceres and Kosik, 1990; DiTella et al., 1996). For all the experiments the antisense oligonucleotides were preincubated with 2  $\mu$ l of lipofectin reagent (1 mg/ml; GIBCO BRL, Gaithersburg, MD) diluted in 100  $\mu$ l of serum-free medium. The resulting oligonucleotide suspension was then added to the NGF-treated PC12 cells at concentrations ranging from 1–5  $\mu$ M. Control cultures were treated with the same concentration of the corresponding sense-strand oligonucleotides. For some experiments, PC12 cells were treated for 1 d with a nonmodified KHC antisense oligonucleotide designated  $-11/+14$  hkin (Ferreira et al., 1992, 1993; Feiguin et al., 1994) in order to suppress KHC expression; this antisense oligonucleotide was used at a concentration of 50  $\mu$ M.

The administration of all oligonucleotides was as follows: after PC12 cells have differentiated in the presence of NGF for 3 d, the oligonucleotides were added to the culture medium. The medium was then supplemented with additional oligonucleotide every 12 h until the end of the experiment.

### Primary Antibodies

The following primary antibodies were used in this study: an mAb against all isoforms of  $\beta$ -tubulin (clone DM1B, mouse IgG; Sigma Chemical Co., St. Louis, MO) diluted 1:100; an mAb against tyrosinated  $\alpha$ -tubulin (clone TUB-1A2, mouse IgG; Sigma Chemical Co.) diluted 1:2,000; an mAb against KHC (clone SUK4; Ingold et al., 1988) diluted 1:10; an mAb against synaptophysin (clone SY38, mouse IgG; Boehringer Mannheim Biochemicals) diluted 1:100; an mAb against GAP-43 (clone 9-1E12; Gosselin and Banker, 1990) diluted 1:1,000; an mAb against the amyloid precursor protein (Boehringer Mannheim Biochemicals) diluted 1:50; an mAb against N-cadherin (clone GC4; Sigma Chemical Co.) diluted 1:100; an affinity-purified rabbit polyclonal antibody against synapsin I (a generous gift of Dr. A. Ferreira) diluted 1:50; and an affinity-purified rabbit polyclonal antibody against  $\beta_{gc}$  (Quiroga et al., 1995; Mascotti et al., 1997) diluted 1:100. In addition, we generated two peptide antibodies against KIF2. One peptide corresponds to amino acid residues 526–535 of mouse KIF2, while the other corresponds to amino acids 114–123 of the same KIF2 molecule. The peptides were coupled to keyhole limpet hemocyanin (KLH; Sigma Chemical Co) using glutaraldehyde as cross-linker. After emulsification with Freund's adjuvant (GIBCO BRL, Gaithersburg, MD), the resultant compounds were injected into rabbits at doses of 0.5 mg. On the third day after the third booster, the rabbits were bled from the ear, the serum was then affinity purified using a protein A column.

### Western Blot Analysis

Equal amounts of crude brain homogenates or whole cell extracts from PC12 cells were fractionated on 7.5% SDS-PAGE and transferred to polyvinylidene difluoride (PVDF) membranes in a Tris-glycine buffer, 20% methanol. The filters were dried, washed several times with TBS (10 mM Tris, pH 7.5, 150 mM NaCl), and blocked for 1 h in TBS containing 5% BSA. The filters were incubated for 1 h at 37° C with the primary antibodies in TBS containing 5% BSA. The filters were then washed three times (10 min each) in TBS containing 0.05% Tween 20, and incubated with a

secondary alkaline phosphatase-conjugated antibody (ProtoBlot Western Blot Alkaline Phosphatase System; Promega Corp., Madison, WI) for 1 h at 37°C. After five washes with TBS and 0.05% Tween 20, the blots were developed with bromochloro-iodolylphosphate (15  $\mu$ l of a 50 mg/ml stock solution) and nitroblue-tetrazolium (2.5  $\mu$ l of a 75 mg/ml stock solution) in 10 ml of alkaline phosphatase detection buffer (100 mM Tris, 100 mM NaCl, 5 mM MgCl<sub>2</sub>, pH 9.5). In addition, KIF2 protein levels were measured by quantitative immunoblotting as described by Drubin et al., 1985 (see also DiTella et al., 1996). For such a purpose, immunoblots were probed with the corresponding primary antibody, followed by incubation with <sup>125</sup>I-protein A. Autoradiography was performed on Kodak X-omat AR film (Eastman Kodak Co., Rochester, NY) using intensifying screens. Autoradiographs were aligned with immunoblots and KIF2 protein levels were quantitated by scintillation counting of nitrocellulose blot slices.

### Preparation of Microtubules from Cytosolic Fractions

For some experiments, microtubules were prepared from cytosolic fractions obtained from the cerebral cortex of 7-d-old rats by the method of Vallee (1982) in the presence or absence of AMP-PNP. The association of KIF2 with microtubules was then evaluated by Western blotting of the microtubule pellet using the anti-KIF2 antibodies. In an additional set of experiments, microtubule pellets were incubated with 10 mM ATP and 100 mM NaCl to release KIF2 from the microtubules. The presence of KIF2 in the supernatant was also assessed by Western blotting.

### Subcellular Fractionation and Sucrose Density Gradient Centrifugation

Multiple fractions from 3-d-old rat cerebral cortex were prepared according to standard procedures (see Ueda et al., 1979; Kondo et al., 1994). Briefly, rat cerebral cortex was gently homogenized with 10 $\times$  vol of ice-cold 0.32 M sucrose, 10 mM Hepes, pH 7.4. The homogenate was centrifuged at low speed (3,000 g) for 10 min at 4°C. The supernatant was centrifuged at medium speed (9,200 g) for 15 min. The medium speed supernatant was again centrifuged at high speed (100,000 g) for 60 min to yield a cytosolic fraction (Fig. 1, S3) and a microsomal one (Fig. 1, P3). All the obtained fractions (supernatants and pellets) were then subjected to electrophoresis, transferred to PVDF membranes, and probed with the antibodies against KIF2. For some experiments, the microsomal fraction was further applied to a 0.3–1.6 M sucrose density gradient at 48,000 rpm for 2 h in a Sorvall STS 60.4 rotor (Sorvall Instruments, Newtown, CT). 0.3-ml fractions were collected from 4-ml tubes; they were then centrifuged at 100,000 g, and the resulting pellets resuspended in Laemmli buffer. The same volume from each fraction was applied to SDS-PAGE and transferred to PVDF membrane. Fractions were then analyzed by immunoblotting with antibodies against KIF2, KHC, synaptic vesicle markers, and growth cone membrane components.

### Immunoisolation of KIF2-containing Organelles

Immunoisolation of KIF2-containing organelles was performed as described by Okada et al. (1995). Thus, for this experiment anti-KIF2 antibodies were covalently attached to protein A–Sepharose beads via dimethylpimelumidate. Microsomal fractions were incubated with these beads at 4°C for 6 h, and the beads were recovered by centrifugation (5,000 rpm for 120 s), and washed with 20 mM Hepes, 100 mM K-aspartate, 40 mM KCl, 5 mM EGTA, 5 mM MgCl<sub>2</sub>, 2 mM Mg-ATP, 1 mM DTT, pH 7.2, supplemented with several protease inhibitors. The supernatant was spun down (75,000 rpm for 30 min) to collect the remaining organelles. Immunoblotting was then performed as previously described with antibodies against  $\beta_{\text{gc}}$ , KHC, synaptophysin, synapsin I, and amyloid precursor protein (APP).

### Immunofluorescence

Cells were fixed before detergent extraction and processed for immunofluorescence as previously described (DiTella et al., 1996). The antibody staining protocol entailed labeling with the first primary antibody, washing with PBS, staining with labeled secondary antibody (fluorescein- or rhodamine-conjugated) and washing similarly; the same procedure was repeated for the second primary antibody. Incubations with primary antibodies were for 1 or 3 h at room temperature, while incubations with secondary antibodies were performed during 1 h at 37°C. The cells were observed with an inverted microscope (Axiovert 35M; Carl Zeiss, Inc.,

Thornwood, NY) equipped with epifluorescence and differential interference contrast (DIC) optics and photographed using either a  $\times 40$ , a  $\times 63$  or  $\times 100$  objective (Carl Zeiss, Inc.) with Tri X-Pan or T-MAX 400 ASA film (Eastman Kodak Co.). Exposures times ranged from 45 to 60 s.

### Morphometric Analysis of Neuronal Shape Parameters

Images were digitized on a video monitor using Metamorph/Metafluor software (Image Universal Co.). To measure neurite length, fixed, unstained, or antibody-labeled cells were randomly selected and traced from a video screen using the morphometric menu of the Metamorph as described previously (DiTella et al., 1996). All measurements were performed using DIC optics at a final magnification of  $\times 768$ . Differences among groups were analyzed by the use of ANOVA and Student-Newman Keuls test.

## Results

### Characterization of the Peptide Antibodies Against KIF2

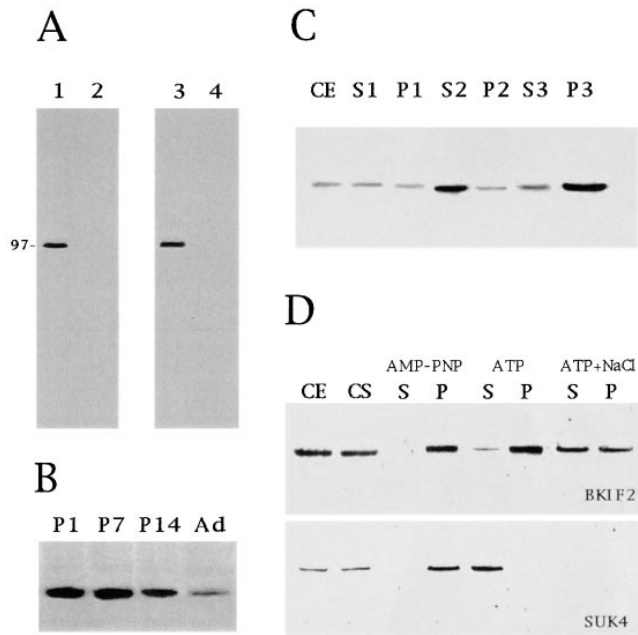
The monospecificity of the affinity-purified rabbit polyclonal antibody (BKF2) raised against a peptide corresponding to amino acid residues 526–535 of mouse KIF2 is shown in Fig. 1 A. This antibody recognizes a single band of  $\sim 97$  kD in Western blots of whole cell homogenates from the cerebral cortex of developing rats (Fig. 1 A, lane 1); an identical staining pattern is observed when equivalent blots are reacted with RKF2, a rabbit polyclonal antibody raised against a peptide corresponding to amino acid residues 114–123 of the KIF2 molecule (Fig. 1 A, lane 3). The staining generated by these antibodies is completely abolished by neutralization with the corresponding purified peptides (Fig. 1 A, lanes 2 and 4).

Fig. 1 B shows that in the cerebral cortex the expression of the BKF2 immunoreactive protein species is higher at early postnatal days, declining gradually but considerably until adulthood, where the lowest levels are detected. In addition, Western blot analysis of subcellular fractions obtained from the cortex of 3-d-old rats revealed that the 97-kD protein is relatively concentrated in the microsomal fraction compared with the cytosol or the mitochondrial fraction (Fig. 1 C). This means that a considerable amount of the protein recognized by the BKF2 antibody is associated with small membranous organelles, but only barely associated with larger ones such as mitochondria (Fig. 1 C). In addition, microtubule binding experiments show that in the absence of ATP, the 97-kD protein cosediments with taxol-stabilized microtubules obtained from the cerebral cortex (Fig. 1 D). This binding occurs in the presence (Fig. 1 D) or absence (not shown) of AMP-PNP; on the other hand, the 97-kD protein is released from microtubules incubated with 10 mM ATP plus 100 mM NaCl, but not in the presence of ATP alone (Fig. 1 D).

Since all the properties described above are identical to those previously reported for KIF2 (see Noda et al., 1995), we conclude that our antibodies effectively recognize KIF2 and not a different protein having a similar molecular weight.

### Subcellular Distribution of KIF2

To begin analyzing the type of cargo that KIF2 may transport, microsomal fractions from rat cerebral cortex were fractionated by isopycnic sucrose density gradient centrifuga-



**Figure 1.** (A) Specificity of the affinity-purified peptide antibodies against KIF2 as revealed by Western blot analysis of whole tissue extracts from the cerebral cortex of 3-d-old rats reacted with the BKF2 (diluted 1:100; lane 1), or RKF2 (diluted 1:100; lane 3). Both antibodies stain a single immunoreactive protein species with an apparent molecular weight of 97 kD. The staining generated by these antibodies is completely abolished by neutralization with the corresponding purified peptides (lanes 2 and 4). 20  $\mu$ g of total protein was loaded in each lane. (B) The expression of KIF2 in the developing rat cerebral cortex as revealed by immunoblot analysis of whole tissue extracts. *P1–P14*, Post-natal d 1–14; *Ad*, adult. KIF2 is highly expressed in the developing cerebral cortex. The blot was reacted with RKF2 (dilution 1:100); 40  $\mu$ g of total protein were loaded in each lane. (C) Western blot analysis of subcellular fractions obtained from the cerebral cortex of 3-d-old rats showing that KIF2 is highly enriched in the microsomal fraction (*P3*). *CE*, crude extract; *S1*, low speed supernatant; *P1*, pellet 1; *S2*, medium speed supernatant; *P2*, pellet 2; *S3*, high speed supernatant; *P3*, pellet 3 or microsomal fraction. The blot was reacted with RKF2 (dilution 1:100); 20  $\mu$ g of protein was loaded in each lane. (D) KIF2 precipitates with microtubules prepared from cytosolic fractions of developing rat cerebral cortex by the method of Vallee (1982; see Materials and Methods). The presence of KIF2 or KHC in the microtubule pellet was then assessed by Western blotting with the BKF2 (dilution 1:25) or SUK4 (dilution 1:100) antibodies. *CE*, crude extract; *CS*, cytosolic fraction; *S*, supernatant after microtubule pelleting in the presence of AMP-PNP; *P*, microtubule pellet obtained in the presence of AMP-PNP; *S*, supernatant fraction after microtubule pelleting in the presence of ATP (10 mM); *P*, microtubule pellet in the presence of ATP (10 mM); *S*, supernatant fraction after microtubule pelleting in the presence of ATP (10 mM) plus NaCl (100 mM); *P*, microtubule pellet in the presence of ATP (10 mM) plus NaCl (100 mM). Note that KIF2, as opposed to KHC, is only slightly released from microtubules in the presence of ATP.

gation and analyzed by immunoblotting with antibodies against KIF2, KHC, and several membrane proteins, including synaptic and nonsynaptic vesicle constituents. This type of approach has already proven useful to identify the type of membrane-bound organelle transported by KIF1A, another member of the kinesin superfamily (Okada et al., 1995).

Approximately 70–80% of KIF2 and KHC were recovered in the P3 (high speed pellet) fraction, while <30% were present in the P2 (medium speed fraction) and S3 (high speed supernatant) fractions. In the P3 microsomal fraction, KHC was recovered in a fraction that extends from 0.3 to 0.6 M sucrose (Fig. 2). By contrast, KIF2 was recovered in a different fraction extending from 0.4 to 0.9 M sucrose, with a peak at 0.6–0.8 M sucrose (Fig. 2). The distribution of KIF2 across the sucrose density gradient was then compared with that of synaptophysin and synapsin I, two well-characterized synaptic vesicle (SV) membrane proteins (Fletcher et al., 1991). The results obtained showed that synaptophysin was recovered in lighter fractions (0.3–0.6 M) than those enriched in KIF2, while synapsin I was recovered in fractions extending from 0.6 to 1.0 M sucrose (Fig. 2). The staining for synapsin I overlapped with that of KIF2, but the peak fractions were different.

Next we compared the distribution of KIF2 with that of three well-characterized growth cone membrane compo-

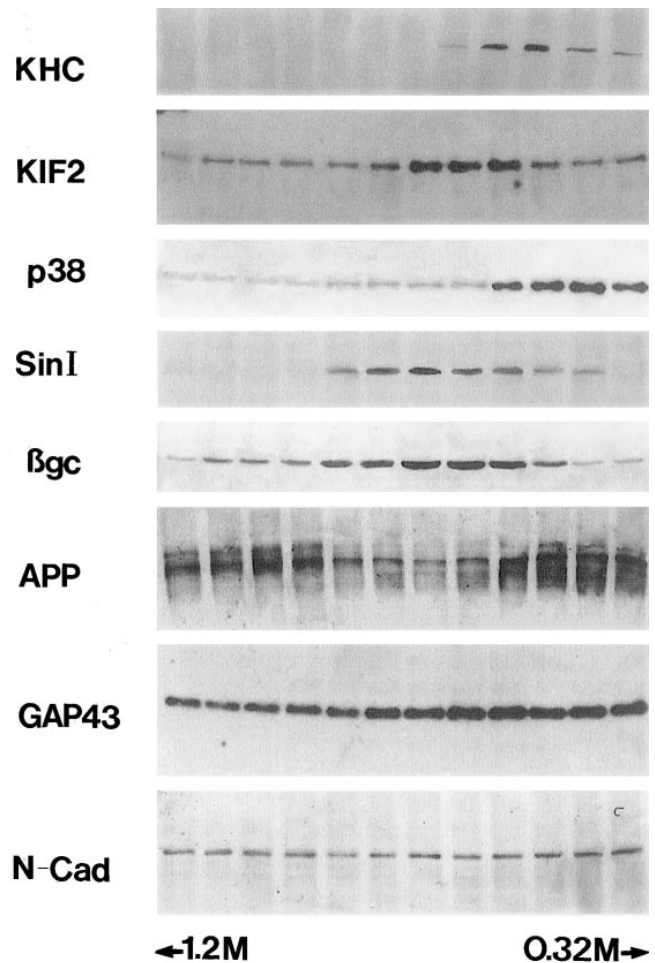


**Figure 2.** The binding of KIF2 to membrane vesicles. Microsomal fraction from developing rat cerebral cortex was fractionated by sucrose gradient centrifugation, and the same volume from each fraction was applied to SDS-PAGE, transferred to PVDF membranes, and analyzed by immunoblotting with antibodies against KHC, KIF2, synaptophysin (*p38*), synapsin I (*Sin I*),  $\beta_{gc}$ , APP, GAP43, and N-cadherin (*N-Cad*). Note that the peak fractions of KIF2 and  $\beta_{gc}$  are highly coincident.

nents. One of them, designated  $\beta_{gc}$  (a novel variant of the  $\beta$ -subunit of the IGF-1 receptor, which is highly enriched in growth cone membranes; Quiroga et al., 1995; Mascotti et al., 1997), displayed a striking codistribution with KIF2, being highly enriched in the 0.6–0.8 M sucrose fractions (Fig. 2). On the other hand, GAP-43 (Goslin et al., 1989) and APP (Ferreira et al., 1993; Yamazaki et al., 1995b) distributed across the sucrose gradient with a pattern clearly different from that of KIF2 (Fig. 2). Thus, GAP-43 was recovered in all fractions of the sucrose gradient (0.3–1.6 M), while APP was enriched in either lighter (0.3–0.6 M) or heavier (1.0–1.6 M) fractions than those containing KIF2. The pattern of distribution of N-cadherin, a cell-adhesion molecule, was also compared with that of KIF2; this protein displayed a uniform distribution across the sucrose gradient, showing no enrichment in the fractions containing KIF2 or  $\beta_{gc}$  (Fig. 2).

Taken collectively, these observations confirm previous studies suggesting the existence of at least two classes of organelles that contain SV membrane proteins: one contains synapsin I, and the other synaptophysin (Okada et al., 1995). The former appears to be transported by KHC (Ferreira et al., 1992), while the latter by KIF1A (Okada et al., 1995). Our observations also suggest the existence of another type of organelle that appears to contain a nonsynaptic growth cone membrane component, namely  $\beta_{gc}$ , and KIF2. However, because other KIFs (KHC, KIF1A, and KIF3; Kondo et al., 1994; Okada et al., 1995) are also present in these fractions, definite conclusions cannot be drawn on the motor for the  $\beta_{gc}$ -containing organelles. Besides, the relationship between synaptophysin- and synapsin I-containing organelles with the ones enriched in KIF2 is also unclear, given that some degree of overlap exists among the fractions containing these proteins. Therefore, to clarify some of these points and directly determine the relationship between KIF2 and  $\beta_{gc}$ , immunoisolation of organelles from the microsomal fraction was performed with antibodies against KIF2. The remaining organelles were recovered by pelleting from the supernatant fraction. Fig. 3 shows that with this method, the KIF2-containing organelles were quantitatively collected. In this immunoisolated organelle fraction  $\beta_{gc}$  was quantitatively recov-

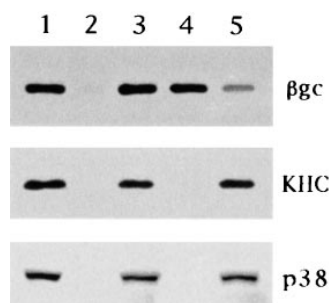


**Figure 3.** Immunoisolation of  $\beta_{gc}$ -containing organelles with the BKF2 antibody (dilution 1:20). Lane 1, microsome fraction before immunoprecipitation. Lanes 2 and 3, microsome fraction incubated with BKF2 preimmune serum—pellet (lane 2) and remanent organelles (lane 3). Lanes 4 and 5, microsome fraction incubated with BKF2—pellet (lane 4)

and remanent organelles (lane 5). Each of these fractions was applied to SDS-PAGE, transferred to PVDF membranes, and analyzed by immunoblotting with antibodies against  $\beta_{gc}$ , KHC, or synaptophysin. Note that  $\beta_{gc}$ , but not KHC or synaptophysin (*p38*) is quantitatively recovered in the immunisolated fraction (lane 4); only a faint band is detected in the remanent organelle fraction (lane 5).

ered (Fig. 3A). In contrast, KHC (Fig. 3B), synaptophysin (Fig. 3C), or synapsin (not shown) were not, or were only slightly detectable in this fraction. These proteins were quantitatively recovered in the remaining organelle fraction. They were not detected in the supernatant fraction after pelleting the remaining organelles, effectively ruling out the possibility that the lack of these proteins in the KIF2 organelle-containing fraction was due to dissociation during the immunoisolation procedure.

These results clearly and directly demonstrate that KIF2 is associated with a class of nonsynaptic, membranous organelle that contains  $\beta_{gc}$  as one of its components. However, they do not provide evidence about the *in vivo* relationship between KIF2 expression and the transport of  $\beta_{gc}$ -containing organelles, and/or the functional role of KIF2 during neuronal morphogenesis. Therefore, to obtain evidence about these aspects we decided to examine the pattern of expression and subcellular distribution of KIF2, as well as the consequences of KIF2 suppression on the distribution of  $\beta_{gc}$  in PC12 cells. In this cell system,  $\beta_{gc}$  expression is upregulated by NGF and highly correlated with neurite outgrowth. Even more importantly, in NGF-treated PC12 cells,  $\beta_{gc}$  is selectively concentrated in the proximal growth cone region in vesicle-like structures, clearly different from those containing synaptophysin or synapsin I (Mascotti et al., 1997), a phenomenon that also suggests that  $\beta_{gc}$  may be transported to the growth cone area by a motor different from KHC or KIF1A.

#### **The Expression and Subcellular Localization of KIF2 in NGF-treated PC12 Cells**

PC12 cells have proven to be an excellent model system for studying growth cone formation, neurite outgrowth, and the expression of structural and membrane proteins involved in nerve cell morphogenesis (Drubin et al., 1985; Greene et al., 1987; Bearer, 1992; Ezmaeli-Azad et al., 1994; Mascotti et al., 1997). In the absence of NGF, PC12 cells have a round morphology with no neurites or growth cone-like structures. Upon stimulation with NGF, they extend several neurites tipped by well-defined growth cones, which are highly enriched with several SV and non-SV membrane markers, such as synaptophysin and  $\beta_{gc}$  (Mascotti et al., 1997).

Fig. 4 shows that NGF induces the expression of KIF2 in PC12 cells (Fig. 4, lanes 1 and 2). Thus, only one band of about 100 kDa  $M_r$  is detected when whole cell extracts from PC12 cells, cultured for 72 h in the presence of NGF, are resolved in SDS-PAGE, blotted and immunostained with the anti-KIF2 antibodies (Fig. 4, lane 2). At equivalent, or even two to threefold higher protein loadings, KIF2 is barely detectable in cell extracts from PC12 cells cultured without NGF (Fig. 4, lane 1). In addition, if NGF-differentiated (4 d) PC12 cells are deprived of the neurotrophin for 6–12 h, neurite length decreases significantly (see Mascotti et al., 1997), as do KIF2 protein levels (Fig. 4, lane 3). These results showed that, in PC12 cells KIF2 expression (as in the case of  $\beta_{gc}$ ; Mascotti et al., 1997) is tightly controlled by NGF as well as differentiation.

In the next series of experiments the spatial distribution of KIF2 was studied by double immunolabeling with the BKF2 antibody and an mAb that recognizes tyrosinated

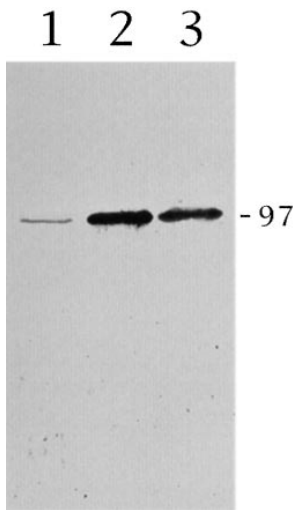


**Figure 4.** KIF2 expression in PC12 cells. Immunoblot analysis of whole cell extracts from nontreated (lane 1) or NGF-treated (lane 2) PC12 cells reacted with the BKF2 antibody (dilution 1:50). NGF induces the expression of a single KIF2 immunoreactive protein species with an apparent molecular mass of 97 kD. Note that KIF2 is barely detected in undifferentiated PC12 cells. When NGF-differentiated PC12 cells were deprived of the neurotrophin for 6 h, KIF2 becomes considerably less abundant (lane 3) than in control ones (lane 2). 40  $\mu$ g of protein were loaded in each lane and the immunoblots were revealed using a rabbit Proto-Blot (Promega) staining kit. PC12 cells were treated with NGF (50 ng/m) for 3 d.

$\alpha$ -tubulin (clone TUA 1.2). PC12 cells cultured in the absence of NGF have a round or polygonal morphology (Fig. 5 A, tubulin antibody), and exhibit very weak immunofluorescence when incubated with the KIF2 antibody (Fig. 5 B). As expected, a significant increase in KIF2 immunofluorescence becomes evident when PC12 are cultured in the presence of NGF. This phenomenon is detected  $\sim$ 48 h after the addition of NGF, when PC12 cells begin to acquire a neuron-like morphology. At this stage, the cells have several short neurites tipped with small growth cones. KIF2 immunofluorescence is preferentially localized to the perinuclear region and to the growth cones (Fig. 5 D; compare with tubulin staining in Fig. 5 C). An exception is the occasional short neurites that contain a continuous band of granular staining between the perinuclear region and the growth cones. After 72 h in the presence of NGF, PC12 cells have extended several long neurites that ended in prominent growth cones. At this stage KIF2 immunostaining has become very intense within the growth cone area, but has disappeared completely from neuritic shafts; a similar pattern is detected in PC12 cells cultured with NGF for longer periods of time (3–7 d). Observation of the growth cones at high magnification demonstrates that KIF2 staining labels a punctate organelle pattern (Fig. 5, E and F).

#### **Antisense Oligonucleotides Affect KIF2 Expression**

Three phosphorothioate (S-modified) antisense oligonucleotides were tested for their ability to inhibit KIF2 expression. PC12 treated with NGF for 3 d and incubated for 24 h with each of the antisense oligonucleotides (5  $\mu$ M dose) described in Materials and Methods show markedly reduced reactivity to the RKF2 antibody, as assessed by Western blotting of whole cell extracts (Fig. 6 A; Table I). In contrast, cells treated with sense oligonucleotides are comparable in their immunoreactivity to untreated control cells (Fig. 6 A). Exposure to the antisense oligonucleotides

did not affect tubulin (Fig. 6 A), KHC (Fig. 6 B), dynein (not shown),  $\beta_{gc}$  (Fig. 6 C), or synaptophysin (Fig. 6 D) immunoreactivity by the same assay. The presence of normal levels of these proteins in the KIF2-suppressed cells suggests that the effect of the antisense treatment is specific and that the regulation of the expression of other motor proteins (e.g., KHC or dynein) is independent of KIF2.

#### **Distribution of $\beta_{gc}$ in Antisense-treated Neurons**

Next we examined the distribution of  $\beta_{gc}$ , synaptophysin, synapsin I, GAP-43, and APP in control and KIF2 antisense oligonucleotide-treated PC12 cells. As expected, KIF2 immunofluorescence is significantly reduced in differentiated PC12 cells treated with the ASKF2a or ASKF2b antisense oligonucleotides (not shown). A dramatic alteration in the distribution of  $\beta_{gc}$  is also detected (Fig. 7). Thus, while in nontreated or sense-treated differentiated control PC12 cells  $\beta_{gc}$  is selectively and highly enriched at growth cones (Fig. 7, A and B), in the KIF2 antisense-treated cells, all of the labeling is present within the cell body, being completely absent from neuritic shafts including their tips (Fig. 7, C–F). By contrast, the distribution of synaptophysin, synapsin I, APP, and GAP-43 is unaltered in the KIF2 antisense-treated cells when compared with that observed in the control cells (nontreated or sense-treated); thus, all of these proteins are highly concentrated within the perinuclear region, presumably the Golgi complex, and the growth cones (Figs. 8, A–H, and 9, A and B).

To determine if other motors may participate in  $\beta_{gc}$  transport, cells were treated with KHC antisense oligonucleotides. As shown in Fig. 9, KHC suppression does not alter the distribution of  $\beta_{gc}$  (Fig. 9, C and D); however, and as previously described (see Ferreira et al., 1993; Yamazaki et al., 1995b) this treatment produces a dramatic reduction of APP immunolabeling at the growth cone and a concomitant accumulation within the cell body (Fig. 9, C and D).

#### **Effect of KIF2 Antisense Oligonucleotides on Neurite Extension**

During the course of these experiments it became evident that one additional effect of KIF2 suppression was a reduction in the length of PC12 neurites. Therefore, to precisely examine this effect, neurite extension was measured in NGF-treated PC12 cells after either a 24- or a 36-h exposure to the KIF2 antisense oligonucleotides. When PC12-treated with NGF for 3 d are exposed to the ASKF2a antisense oligonucleotide (5  $\mu$ M) and fixed 24 h later there is a slight decrease in neurite length. In the antisense-treated cultures, the mean total neurite length per cell is  $225 \pm 5 \mu\text{m}$ , a value lower than that observed in control ( $260 \pm 8 \mu\text{m}$ ) or sense-treated ( $265 \pm 8 \mu\text{m}$ ) cells. Neurite length in neurons exposed to KIF2 antisense oligonucleotides (5  $\mu$ M) for 36 h is quantitated in Table II. These cells exhibit a 60–70% decrease in neurite length. Our observations also show that the KIF2 antisense oligonucleotides affected neurite outgrowth in a dose-dependent manner; thus, at 2.5  $\mu$ M the total neurite length was reduced 35% and at 1  $\mu$ M it was only reduced 15% (Table II). While suppressing KIF2 expression, the KIF2 antisense oligonucleotides did not irreversibly damage the neurons. When, after 36 h in the presence of the antisense

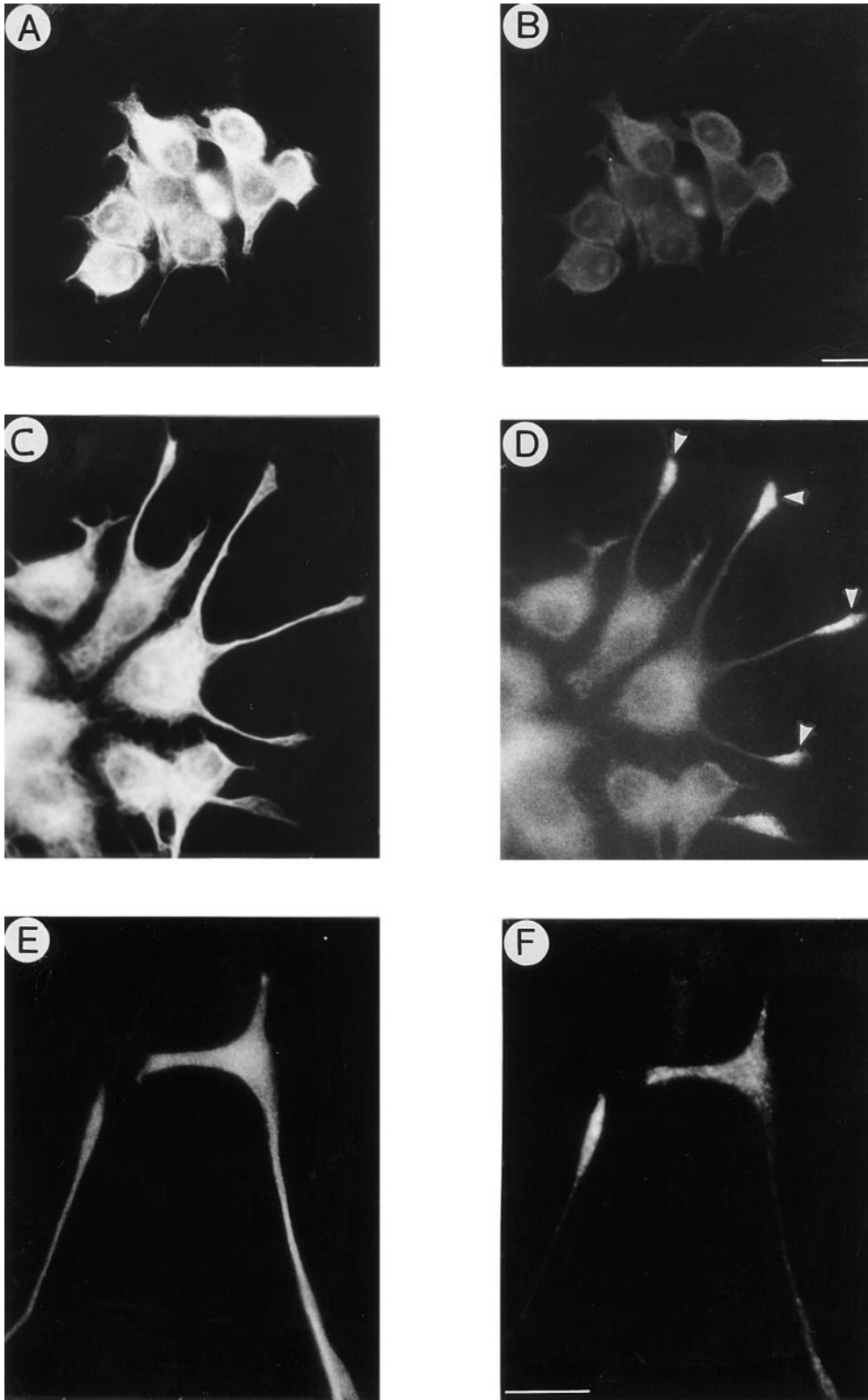


**Figure 5.** KIF2 becomes localized to growth cones in differentiated PC12 cells. Double immunofluorescence micrographs showing the distribution of tyrosinated  $\alpha$ -tubulin (A, C, and E) and KIF2 (B, D, and F) in PC12 cells. PC12 cells, cultured in the absence of NGF, display low positive immunofluorescence for the RKF2 antibody (A and B). A dramatic increase in KIF2 immunofluorescence is detected in PC12 cells treated with NGF for 2 d. In these cells, KIF2 is localized to the perinuclear region and highly enriched in growth cones (arrowheads). High power micrographs of neuritic tips reveal a granular (vesicle-like) appearance of the KIF2 immunostaining (F). Bars: 10  $\mu$ m.

oligonucleotides, the cells are released from antisense inhibition by changing the medium, neurite extension resumed at a rate that paralleled that observed under control conditions (see below).

In the final set of experiments, we used quantitative fluorescence and the morphometry of fixed cells to analyze

expression of KIF2 and compare it with both the time course of  $\beta_{gc}$  disappearance from the growth cone area, and the reduction of neurite length in PC12 cells treated with the ASKF2a antisense oligonucleotide for different periods of time. The results obtained show that the decrease in KIF2 immunofluorescence precedes the disap-



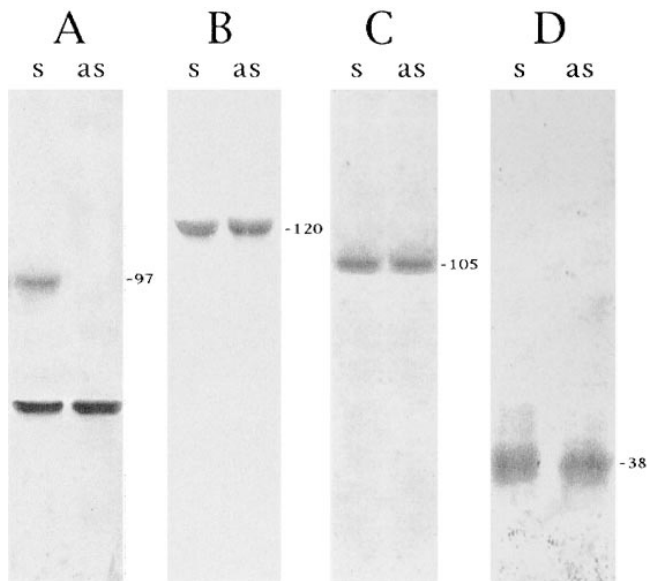


**Figure 6.** Effect of the KIF2 antisense oligonucleotide ASKF2a (5  $\mu$ M) on KIF2 (A), tyrosinated  $\alpha$ -tubulin (A), KHC (B),  $\beta_{gc}$  (C), and synaptophysin (D) protein levels as revealed by Western blot analysis of whole cell homogenates obtained from PC12 cells. For this experiment PC12 cells cultured in the presence of NGF were treated for 24 h with the ASKF2a oligonucleotide. Antisense treatment was initiated 3 d after the addition of NGF (50 ng/ml). Control cultures were treated with equivalent doses of sense oligonucleotides. (A) Blot reacted with antibodies against KIF2 (RKF2 diluted 1:50) and tyrosinated  $\alpha$ -tubulin (mAb TUB-1A2), or with mAb SUK 4 (B), or with an affinity-purified polyclonal antibody against  $\beta_{gc}$  (C), or with mAb SY38 (D). 30  $\mu$ g of total cellular protein were loaded in each lane. Blots were revealed using the ProtoBlot staining kit (Promega).

pearance of  $\beta_{gc}$  from the growth cone area, a phenomenon which in turn precedes the decrease in neurite length by several hours (Fig. 10, A and B). Similarly, when the cells are released from the antisense treatment the reexpression of KIF2 precedes the redistribution of  $\beta_{gc}$  to the growth

**Table I.** Effect of KIF2 Antisense Oligonucleotides on KIF2 and Tubulin Protein Levels in NGF-treated PC12 Cells

Group	KIF2	Tubulin
Nontreated	2,750 $\pm$ 200	5,500 $\pm$ 150
Sense-treated		
MKF2-11/+14 (50 $\mu$ M)	2,800 $\pm$ 150	6,000 $\pm$ 180
ASMKF2 (50 $\mu$ M) -11/+14	250 $\pm$ 50*	5,700 $\pm$ 250
Sense-treated SKF2a (5 $\mu$ M)	2,650 $\pm$ 150	5,600 $\pm$ 220
ASKF2a (5 $\mu$ M)	310 $\pm$ 60*	5,850 $\pm$ 120
ASKF2a (2.5 $\mu$ M)	740 $\pm$ 80*	5,700 $\pm$ 150
ASKF2b (5 $\mu$ M)	280 $\pm$ 40*	5,700 $\pm$ 100

PC12 cells were cultured in the presence of NGF (50 ng/ml). On the third day after the addition of NGF, the cells were treated with KIF2 sense or antisense oligonucleotides for a 24-h period.

KIF2 and tubulin protein levels were analyzed by quantitative immunoblotting with  $^{125}$ I-protein A; autoradiographs were aligned with immunoblots, and KIF2 protein levels were quantitated by scintillation counting of nitrocellulose blot slices. 10  $\mu$ g of total cellular protein was used for each sample.

Each value represents the mean  $\pm$  SEM; they are expressed in cpm.

\*Values significantly different from those found in control samples.

cone, a phenomenon which is then followed by an increase in neurite length (Fig. 10, A and B).

## Discussion

### KIF2 and the Subcellular Distribution of $\beta_{gc}$

The present results confirm and extend previous observations by Noda et al. (1995) suggesting that KIF2 is an anterograde microtubule-based motor involved in the transport of a class of nonsynaptic membrane organelles abundant in developing neurons. The new information presented here suggests that at least one of the components transported by KIF2 is  $\beta_{gc}$ , a growth cone nonsynaptic membrane protein (Quiroga et al., 1995; Mascotti et al., 1997). Thus, one striking finding in KIF2-suppressed PC12 cells is the altered distribution of  $\beta_{gc}$ . In untreated cells, or cells treated with sense oligonucleotides,  $\beta_{gc}$  is found selectively concentrated within growth cones. In antisense-treated cells, on the other hand,  $\beta_{gc}$  is confined to the cell body.

Several observations suggest that this effect is the result of a specific and selective blockade of KIF2 expression by the antisense treatment. First, sequence analysis of the regions of the KIF2 mRNAs selected for designing the antisense oligonucleotides reveals no significant homology with any other reported sequence, including other members of the kinesin superfamily. In addition, none of the S-modified antisense oligonucleotides used in this study contains four contiguous guanosine residues, which are believed to increase oligomer affinity to proteins, and hence generate nonspecific antisense inhibitory effects (Wagner, 1995). Secondly, the antisense oligonucleotide treatment dramatically reduces KIF2 protein levels without altering the levels of several other proteins including tubulin, KHC, dynein, synaptophysin, GAP-43, and  $\beta_{gc}$ ; this is important since some of these proteins have been directly implicated in neurite formation (Yankner et al., 1990; Ferreira et al., 1992). Third, the effects of the antisense oligonucleotides are dose dependent and not observed when the cells are treated with equivalent doses of the corresponding sense oligonucleotides. In addition the effects are also observed when the antisense oligonucleotides are used at very low concentrations (2.5  $\mu$ M), a phenomenon which also contributes to rule out the possibility of nonspecific binding of the oligonucleotides to proteins (Wagner, 1995). Fourth, the antisense treatment does not cause irreversible damage to the cells; PC12 cells recover the normal distribution of  $\beta_{gc}$  following a change to medium free of the antisense oligonucleotide. Fifth, KIF2 suppression selectively alters  $\beta_{gc}$  distribution without affecting the subcellular localization of several other growth cone components, including synaptophysin, synapsin I, APP, and GAP-43, which are transported to the neurite terminus by other microtubule-based anterograde motors, such as KIF1A and KHC (Ferreira et al., 1992, 1993; Okada et al., 1995). Conversely, the distribution of  $\beta_{gc}$  is not modified by KHC antisense oligonucleotides, a treatment that significantly disrupts the growth cone localization of APP (Ferreira et al., 1993; Yamazaki et al., 1995b; this study) or GAP-43 (Ferreira et al., 1992).

Several additional lines of evidence also support the



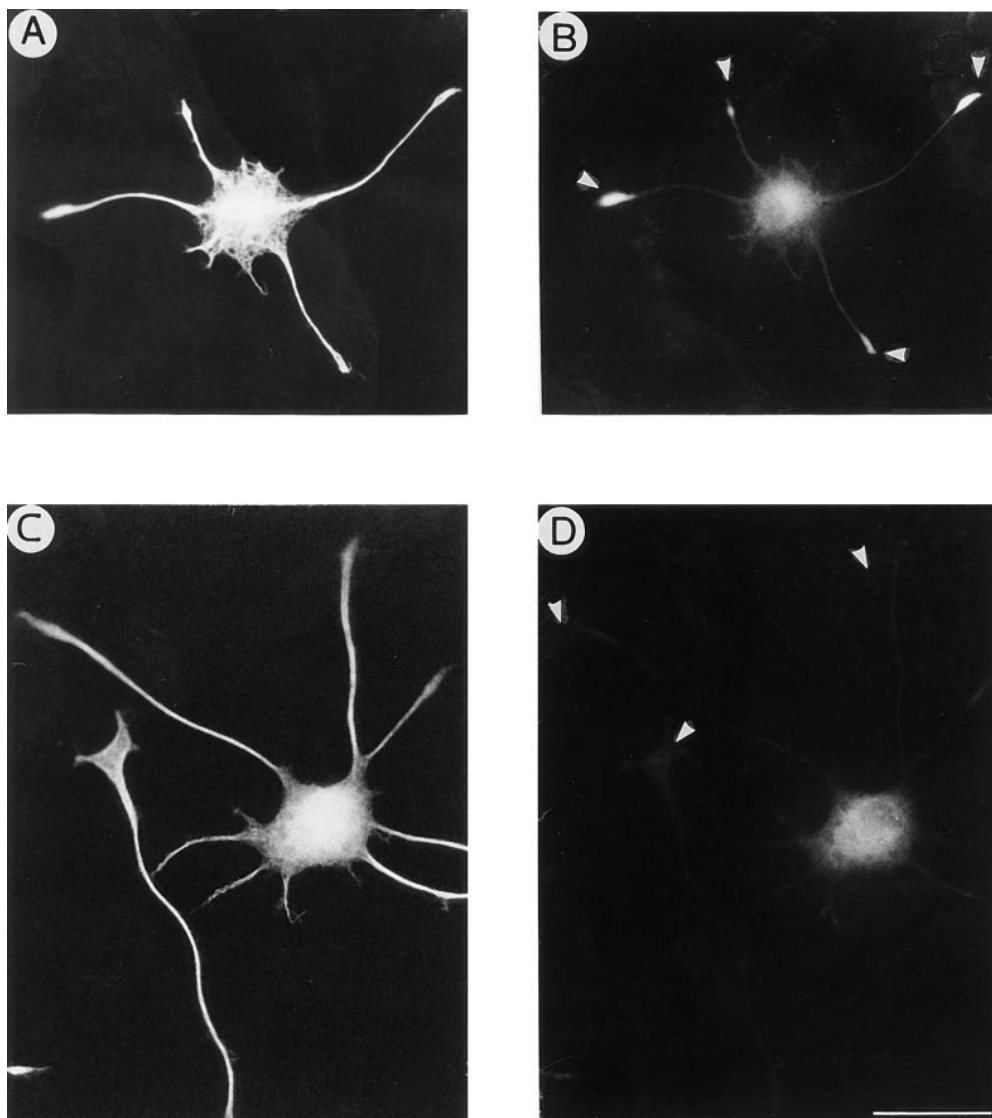


**Figure 7.** KIF2 suppression alters the distribution of  $\beta_{gc}$  in NGF-differentiated PC12 cells. (A and B) Double immunofluorescence micrographs showing tubulin (A) and  $\beta_{gc}$  (B) staining in PC12 cells from a culture treated with a KIF2 sense oligonucleotide (5  $\mu$ M). Note that  $\beta_{gc}$  immunofluorescence is preferentially localized at neuritic tips (arrowheads). (C and D) Double immunofluorescence micrographs showing tubulin (C) and  $\beta_{gc}$  (D) staining in PC12 cells from a culture treated with ASKF2a oligonucleotide (5  $\mu$ M). Note the complete disappearance of  $\beta_{gc}$  from neuritic tips (arrowheads). For these experiments, cells were cultured in serum-free medium in the presence of NGF (50 ng/ml). On day 3, after the addition of NGF, the cells were treated with KIF2 antisense or sense oligonucleotides for a 24-h period; they were then fixed and processed for immunofluorescence as described in Materials and Methods. Bar, 10  $\mu$ m.

idea that KIF2 may serve as the plus-end motor involved in the anterograde transport of  $\beta_{gc}$ -containing vesicles. First, analysis of subcellular fractions obtained by SDG centrifugation of microsomal fractions revealed a striking colocalization of KIF2 with  $\beta_{gc}$ . Second, and even more important, immunisolation experiments allow us to isolate the KIF2 cargo from other organelles and determine that the KIF2 cargo contained  $\beta_{gc}$ , but lacked synaptophysin, synapsin I, and KHC. Third, both KIF2 and  $\beta_{gc}$  are predominantly expressed in developing brain tissue, up-regulated by NGF, and highly enriched in growth cone membrane preparations obtained from fetal brain tissue (Noda et al., 1995; Quiroga et al., 1995). Finally, immunofluorescence studies show that within growth cones  $\beta_{gc}$  associates with a type of vesicle-like structure different from those containing synaptophysin and synapsin I (Mascotti et al., 1997).

The present observations also support the notion that in developing neurons KIF2 function is significantly different from the one performed by other members of the central motor domain subfamily in nonneuronal cells. Thus, all other KIF2-related proteins have been implicated in mito-

sis and spindle elongation (Wordeman and Mitchison, 1995; Walczak et al., 1996). While this seems to be an unexpected finding, it is worth noting that divergence in function among filogenetically related kinesin superfamily members may not be an unusual phenomenon. In fact, a similar situation exists in the case of KIFC2 that, unlike other COOH-terminal kinesin related proteins of the KAR3 family involved in mitosis and meiosis, appears to participate in the retrograde transport of a subpopulation of membrane bound organelles present in neuronal cells (Hanton et al., 1997; Saito et al., 1997). It will now be of considerable interest to begin analyzing the nature of this functional divergence.

#### ***KIF2 Participation in Neurite Extension***

Analysis of the in situ distribution of KIF2 revealed that it is expressed in postmitotic neurons and concentrated in axonal processes of developing neurons (Noda et al., 1995). The present study extends these observations by showing that KIF2 expression is upregulated by environmental factors such as NGF and that its induction profile

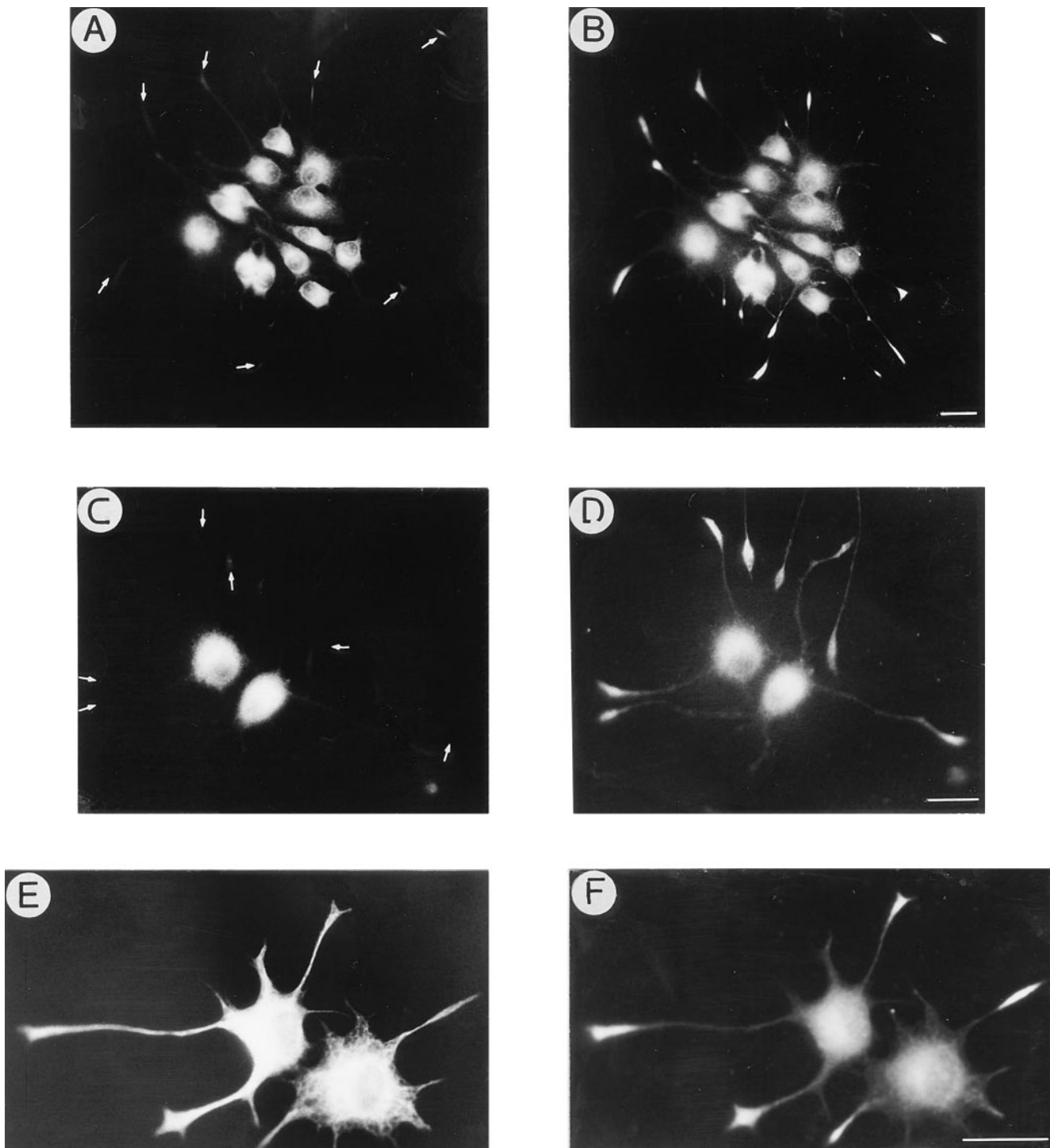


**Figure 8.** KIF2 suppression alters the distribution of  $\beta_{gc}$ , but not of synaptophysin, GAP-43, or synapsin I in NGF-treated PC12 cells. (A–D) Double immunofluorescence micrographs showing the distribution of  $\beta_{gc}$  (A and C), synaptophysin (B), and GAP-43 (D) in NGF-differentiated PC12 cells treated with a KIF2 antisense oligonucleotide (ASKF2a, 5  $\mu$ M). Note that while  $\beta_{gc}$  completely disappears from growth cones (arrows), synaptophysin and GAP-43 remain highly concentrated at neuritic tips. (E and F) Double immunofluorescence micrographs showing the distribution of tyrosinated  $\alpha$ -tubulin (E) and synapsin I (F) in NGF-differentiated PC12 cells treated with ASKF2a (5  $\mu$ M). Note that synapsin I is highly concentrated at neuritic tips. For these experiments, cells were treated with oligonucleotides as described in Fig. 7. Bar, 10  $\mu$ m.

closely parallels neurite extension in PC12 cells. Furthermore, NGF withdrawal not only causes neurite retraction, but also a precipitous drop in KIF2 protein levels. It follows that KIF2 expression is strictly regulated by NGF and

thus, is a differentiation product of PC12 cells; in contrast to KHC, which is expressed in proliferative and non-proliferative cells (Feiguin et al., 1994). The upregulation of KIF2 expression in NGF-treated PC12 cells puts this mol-

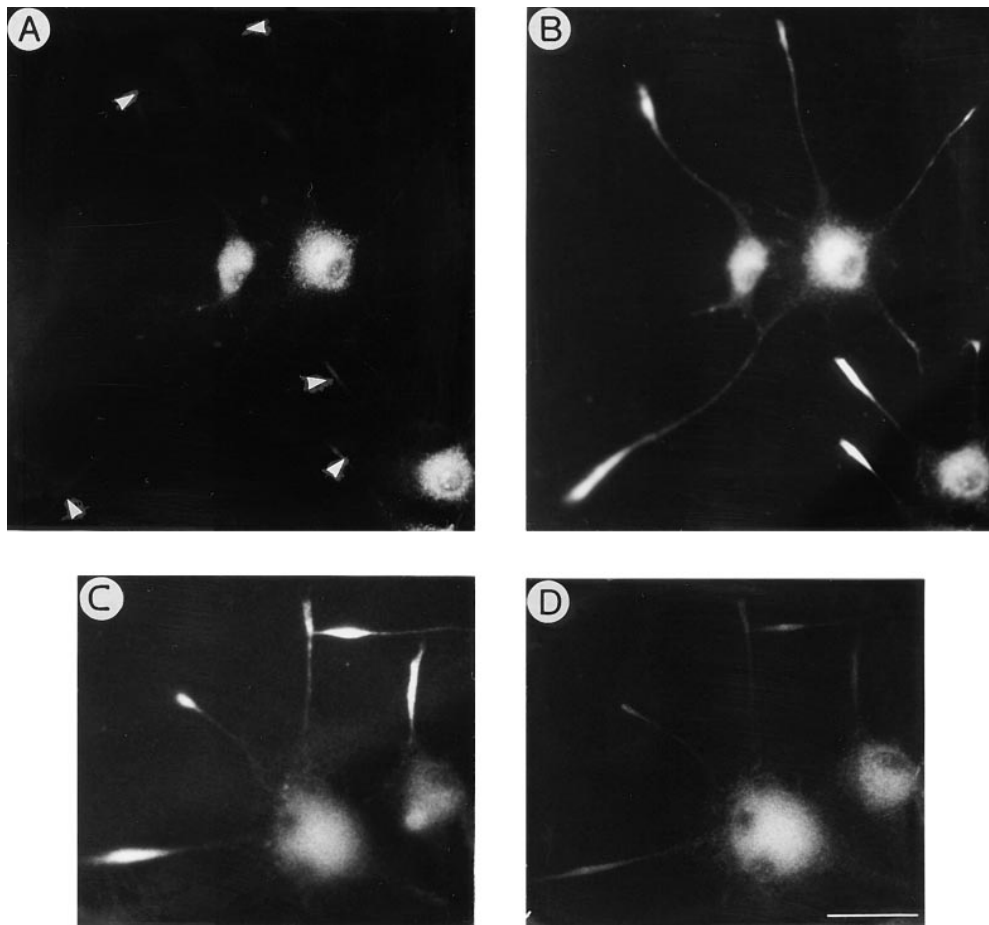


**Figure 9.** (A and B) Double immunofluorescence micrographs showing the distribution of  $\beta_{gc}$  (A) and APP (B) in NGF-differentiated PC12 cells treated with the KIF2 antisense oligonucleotide ASKF2b (5  $\mu$ M). Note that while  $\beta_{gc}$  completely disappears from growth cones (arrowheads) APP remains highly concentrated at neuritic tips. (C and D) Double immunofluorescence micrographs showing the distribution of  $\beta_{gc}$  (C) and APP (D) in NGF-differentiated PC12 cells treated with the KHC antisense oligonucleotide -11/14 hkin (50  $\mu$ M). Note that while this treatment does not affect the growth cone localization of  $\beta_{gc}$ , it dramatically decreases APP immunofluorescence at neuritic tips. For these experiments, cells were treated with antisense oligonucleotides as described in Fig. 7. Bar, 10  $\mu$ m.

ecule in a similar category to MAP1b and tau—two structural MAPs whose expression is induced by NGF (Drubin et al., 1985; Aletta et al., 1988), and that have been directly implicated in neurite extension in PC12 cells (Brugg et al., 1993; Esmali-Azad et al., 1994). The analysis of the phenotype of KIF2-suppressed PC12 cells provides direct evidence about its participation in neurite extension; thus, a

**Table II.** Effect of KIF2 Antisense Oligonucleotides on Neurite Length in NGF-treated PC12 Cells

Group	Mean total neurite length per cell	Number of neurite per cell
Control	295 $\pm$ 8	4.0 $\pm$ 0.2
Sense-treated	310 $\pm$ 6	4.0 $\pm$ 0.3
ASKF2a (5 $\mu$ M)	*110 $\pm$ 5	3.5 $\pm$ 0.3
ASKF2a (2.5 $\mu$ M)	*200 $\pm$ 10	3.8 $\pm$ 0.2
ASKF2b (5 $\mu$ M)	*105 $\pm$ 12	3.4 $\pm$ 0.2
ASKF2b (2.5 $\mu$ M)	*210 $\pm$ 10	3.8 $\pm$ 0.1
ASKF2b (1 $\mu$ M)	260 $\pm$ 14	4.0 $\pm$ 0.1

PC12 cells were cultured in the presence of NGF (50 ng/ml). On the third day after the addition of NGF, the cells were treated with KIF2 sense or antisense oligonucleotides for a 36-h period. They were then fixed and processed for immunocytochemistry (double labeling with tubulin and KIF2 antibodies). Mean total neurite length and the mean number of neurites per cell was evaluated using the morphometric menu of the Metamorph system (see Materials and Methods).

Neurite length values are expressed in  $\mu$ m. A total of at least 250 cells was measured for each experimental condition. Each value represents the mean  $\pm$  SEM.

\*Values significantly different from those found in control cells.

24- or 36- h exposure to KIF2 antisense, but not sense, oligonucleotides results in a significant reduction in neurite length. Interestingly, neurite growth is also impaired in KHC-suppressed neurons, a phenomenon which has been related with the blockade of the anterograde transport of the growth cone regulatory protein, GAP-43 (Ferreira et al., 1992).

While the mechanism(s) by which KIF2 participates in neurite extension are currently unknown, one obvious possibility, as in the case of KHC, relates with the nature and final destination of the cargo that it transports. For example, the KIF2 cargo may contain regulatory proteins that when appropriately delivered to the growth cone will actively participate in neurite outgrowth. Such cargo types may include receptor proteins for certain types of neurotrophic factors, as it might be the case for the  $\beta_{gc}$ -containing IGF-1 receptors. In this regard, one question that arises concerns the possible relationship between the altered distribution of  $\beta_{gc}$  and the inhibition of neurite outgrowth observed in KIF2-suppressed PC12 cells.

IGF-1 appears to function in most cells primarily as a mitogenic peptide, but in the particular case of the developing nervous system it also functions as a neurotrophic factor promoting neurite outgrowth (Aizenmann and De Vellis, 1987; Caroni and Grandes, 1990; Beck et al., 1993; Ishii et al., 1993). The receptor for IGF-1 resembles the insulin receptor, and is a disulfide-linked heterotetrameric ( $\alpha_2\beta_2$ ) transmembrane glycoprotein, with extracellular

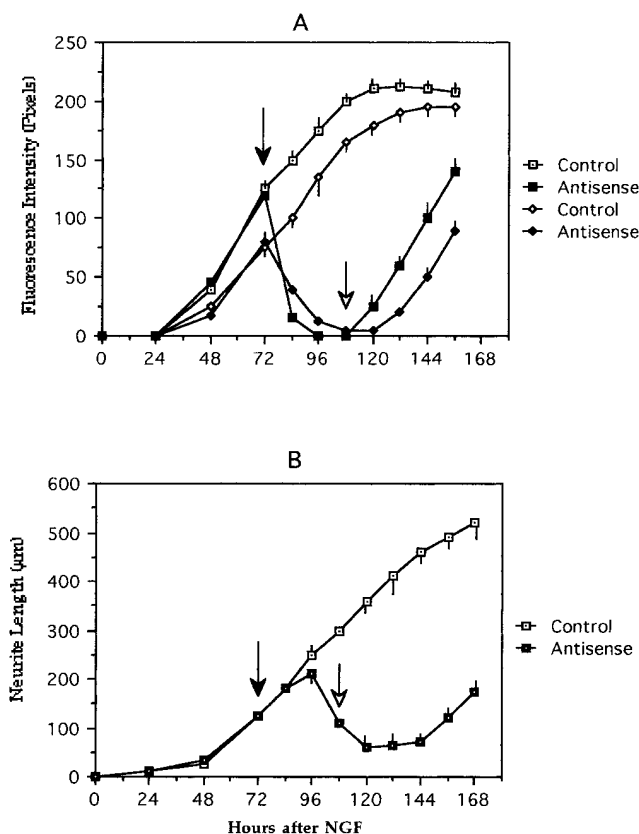


**Figure 10.** (A) Graph showing the effect of the KIF2 antisense oligonucleotide ASKF2a (closed symbols) on KIF2 (squares) and  $\beta_{gc}$  (diamonds) immunofluorescence in NGF-differentiated PC12 cells. After 3 d in the presence of NGF (50 ng/ml), the cells were treated with ASKF2a (5  $\mu$ M; solid arrow) for 36 h; at this time point (open arrow), the medium was changed and the cells maintained in antisense-free medium in the presence of NGF. Control cultures (open symbols) were treated with equivalent doses of the corresponding sense oligonucleotide. KIF2 immunofluorescence was measured in the cell body and growth cones. Only the values obtained from cell body measurements are presented; identical results were obtained from measurements performed within the growth cone area.  $\beta_{gc}$  immunofluorescence was quantitated in the growth cone area. At least 100 cells were measured for each time point and experimental condition. Each value represents the mean  $\pm$  SEM. (B) Graph showing changes in neurite length (mean total neuritic length per cell) in control (sense treated) and KIF2 antisense (ASKF2a, 5  $\mu$ M) oligonucleotide-treated PC12 cells. Each value represents the mean  $\pm$  SEM. A total of 50 cells were measured for each time point and experimental condition. Note that in the antisense-treated cultures the drop in KIF2 and  $\beta_{gc}$  immunofluorescence precedes the reduction of neurite length, and that when cells are released from the antisense treatment the appearance of KIF2 immunofluorescence precedes that of  $\beta_{gc}$  within the growth cone, a phenomenon which is then followed by an increase in neurite length.

ligand-binding ( $\alpha$ ) and intracellular tyrosine kinase ( $\beta$ ) domains (Ullrich et al., 1986). The expression of IGF-1 receptors in the nervous system is high at late embryonic and early postnatal stages and declines significantly afterwards (Ullrich et al., 1986; Werner et al., 1991), again suggesting an important role for this ligand-receptor system in brain development. Interestingly, IGF-1 and its receptor, as well

as KIF2, are expressed permanently in the olfactory bulb where neuronal remodeling and neurite outgrowth continue throughout adult life (Bondy, 1991; Noda et al., 1995); and transgenic mice lacking IGF-1 receptors exhibit serious deficits in neural development (Liu et al., 1993).

In developing neurons, the expression of  $\beta_{gc}$ -containing IGF-1 receptors, but not of other  $\beta$  subunits ( $\beta_{other}$ ) of the insulin or IGF-1 receptors, is correlated with neurite outgrowth, growth cone formation, and (in PC12 cells) is highly dependent on NGF (Mascotti et al., 1997). Taken together, these observations raised the idea that the different functions of IGF-1 (mitogenic or neurotogenic actions) may result from the contrasting regulations and distributions of  $\beta_{gc}$ -containing IGF-1 versus  $\beta_{other}$ -containing insulin/IGF-1 receptors in developing neurons. Thus, an altered distribution of  $\beta_{gc}$ -containing IGF-1 receptors is compatible with the reduction of neurite length observed in KIF2-suppressed neurons. In this regard, it is worth noting that the disappearance of  $\beta_{gc}$  from growth cones precedes the reduction in neurite length; the opposite phenomenon was not observed under the present experimental conditions. However, definite conclusions on this matter will certainly depend on a more detailed characterization of the biological role of  $\beta_{gc}$ -containing IGF-1 receptors as well as of the identification of other components present in the KIF2-transported cargo. Given that other members of the central motor domain subfamily are involved in spindle elongation (Walczak and Mitchison, 1996), it will also be of interest to explore the possible participation of KIF2 in the regulation of microtubule organization and/or dynamics. Studies are in progress to address these and related issues.

This paper is dedicated to NIS and MFM.

The authors express their gratitude to Dr. A. Ferreira for her continuing support.

This work was supported by grants from CONICOR, Fundación Perez-Companc, Fundación Antorchas, and a Fogarty International Collaborative Award (FIRCA). It was also supported by a Howard Hughes Medical Institute grant HMMI 75197-553201 (to A. Cáceres) awarded under the International Research Scholars Program. G. Morfini is a fellow from the National Council of Research from Argentina (CONICET).

Received for publication 6 March 1997 and in revised form 15 May 1997.

## References

- Aizawa, H., Y. Sekine, R. Takemura, Z. Zhang, M. Nangaku, and N. Hirokawa. 1992. Kinesin family in murine central nervous system. *J. Cell. Biol.* 119: 1287-1296.
- Aizenmann, Y., J. De Vellis. 1987. Brain neurons develop in a serum glial free environment: effects of insulin, insulin-like growth factor-I and thyroid hormone on neuronal survival, growth and differentiation. *Brain Res.* 406:32-42.
- Aletta, J.M., S.A. Lewis, N.J. Cowan, and L.A. Greene. 1988. Nerve growth factor regulates both the phosphorylation and steady state levels of microtubule-associated protein 1.2 (MAP1.2). *J. Cell Biol.* 106:1573-1581.
- Bearer, E. 1992. An actin-associated protein present in the microtubule organizing center and the growth cones. *J. Neurosci.* 12:750-761.
- Beck, K., B. Knusel, F. Hefti. 1993. The nature of the trophic action of BDNF, des (1-3) IGF1, and bFGF on mesencephalic dopaminergic neurons developing in culture. *Neuroscience.* 52:855-866.
- Binder, L., A. Frankfurter, H. Kim, A. Cáceres, M. Payne, and L. Rebhun. 1984. Heterogeneity of microtubule-associated protein 2 during rat brain development. *Proc. Natl. Acad. Sci. USA.* 81:5613-5617.
- Bondy, C.A. 1991. Transient IGF-1 gene expression during the maturation of functionally related central projection neurons. *J. Neurosci.* 11:3442-3455.
- Bottenstein, J., G. Sato. 1979. Growth of a rat neuroblastoma cell line in a serum-free supplemented medium. *Proc. Natl. Acad. Sci. USA.* 76:514-517.
- Brady, S.T. 1985. A novel brain ATPase with properties expected for the fast axonal transport motor. *Nature (Lond.).* 317:73-75.
- Brugg, B., D. Reddy, and A. Matus. 1993. Attenuation of microtubule-associ-

- ated protein  $\beta$  expression by antisense oligodeoxynucleotides inhibits initiation of neurite outgrowth. *Neuroscience* 52:489–496.
- Cáceres, A., K. Kosik. 1990. Inhibition of neurite polarity by Tau antisense oligonucleotides in primary cerebellar neurons. *Nature (Lond.)* 343:461–463.
- Caroni, P., P. Grandes. 1990. Nerve sprouting in innervated adult skeletal muscle induced by exposure to elevated levels of insulin-like growth factors. *J. Cell Biol.* 110:267–310.
- DiTella, M., F. Feiguin, N. Carri, K. Kosik, and A. Cáceres. 1996. MAP-1b/Tau functional redundancy during laminin-enhanced axonal growth. *J. Cell Sci.* 109:467–477.
- Drubin, D., S. Feinstein, E. Shooter, and M. Kirschner. 1985. Nerve growth factor-induced neurite outgrowth in PC12 cells involves the coordinate induction of microtubule assembly and assembly promoting factors. *J. Cell Biol.* 101:1799–1807.
- Endow, S. 1991. The emerging kinesin family of microtubule motor proteins. *Trends Biochem. Sci.* 16:221–225.
- Esmaeli-Azad, B., J. McCarty, S.C. Feinstein. 1994. Sense and antisense transfection analysis of tau function: tau influences net microtubule assembly, neurite outgrowth and neuritic stability. *J. Cell Sci.* 107:869–879.
- Feiguin, F., A. Ferreira, K. Kosik, and A. Cáceres. 1994. Kinesin-mediated organelle translocations revealed by specific cellular manipulations. *J. Cell Biol.* 127:1021–1039.
- Ferreira, A., J. Niclas, R.D. Vale, G. Banker, and K. Kosik. 1992. Suppression of kinesin expression in cultured hippocampal neurons using antisense oligonucleotides. *J. Cell Biol.* 117:595–606.
- Ferreira, A., A. Cáceres, and K. Kosik. 1993. Intraneuronal compartments of the amyloid precursor protein. *J. Neurosci.* 13:3122–3133.
- Fletcher, T., P. Cameron, P. DeCamilli, and G. Banker. 1991. The distribution of synapsin I and synaptophysin in hippocampal neurons developing in culture. *J. Neurosci.* 11:1617–1626.
- Goldstein, L.S.B. 1991. The kinesin superfamily: tails of functional redundancy. *Trends Cell Biol.* 1:93–98.
- Goslin, K., and G. Banker. 1990. Rapid changes in the distribution of GAP43 correlate with the expression of neuronal polarity during development and under experimental conditions. *J. Cell Biol.* 110:1319–1331.
- Greene, L., and A. Tischler. 1976. Establishment of a noradrenergic clonal cell line of rat adrenal pheochromocytoma cells which respond to nerve growth factor. *Proc. Natl. Acad. Sci. USA.* 73:2424–2428.
- Greene, L., J. Aletta, A. Rukenstein, and S. Green. 1987. PC12 pheochromocytoma cells: culture, NGF treatment and experimental exploitation. *Methods Enzymol.* 147:207–216.
- Hall, D.H., and E.M. Hedgecock. 1991. Kinesin-related gene unc-104 is required for axonal transport of synaptic vesicles in *C. elegans*. *Cell.* 65:837–847.
- Hanton, D.W., Z. Yang, and L.S.B. Goldstein. 1997. Characterization of KIFC2, a neuronal kinesin superfamily member in mouse. *Neuron.* 18:439–451.
- Hirokawa, N. 1993. Axonal transport and the cytoskeleton. *Curr. Op. Neurobiol.* 3:724–731.
- Hirokawa, N. 1996. Organelle transport along microtubules—the role of KIFs. *Trends Cell Biol.* 6:135–141.
- Hollenbeck, P., and J. Swanson. 1990. Radial extension of macrophage tubular lysosomes supported by kinesin. *Nature (Lond.)* 346:864–866.
- Ingold, A.L., S.A. Cohn, and J.M. Scholey. 1988. Inhibition of kinesin-driven microtubule motility by monoclonal antibodies to kinesin heavy chain. *J. Cell Biol.* 107:2657–2667.
- Ishii, D.N., G.W. Glazner, L.R. Whalen. 1993. Regulation of peripheral nerve regeneration by insulin-like growth factors. *Ann. N.Y. Acad. Sci.* 692:172–182.
- Kondo, S., R. Sato-Yoshitake, Y. Noda, H. Aizawa, Y. Matsuura, and N. Hirokawa. 1994. KIF3A is a new microtubule-based anterograde motor in the nerve axon. *J. Cell Biol.* 125:1095–1115.
- Liu, J.P., J. Baker, A.S. Perkins, E.J. Robertson, and A. Efstratiadis. 1993. Mice carrying null mutations of the gene encoding insulin-like growth factor I (IGF-1) and type 1 IGF receptor (IGF1R). *Cell.* 75:59–72.
- Mascotti, F., A. Cáceres, K. Pfenninger, S. Quiroga. 1996. Expression and distribution of IGF-1 receptors containing a  $\beta$ -subunit variant ( $\beta$ gc) in developing neurons. *J. Neurosci.* 15:1447–1459.
- Mitchison, T., and M. Kirschner. 1988. Cytoskeletal dynamics and nerve growth. *Neuron.* 1:761–772.
- Nakata, T., and N. Hirokawa. 1995. Point mutations of adenosine triphosphate-binding motif generate rigor kinesin that selectively blocks anterograde lysosome membrane transport. *J. Cell Biol.* 131:1039–1053.
- Nangaku, M., Y. Sato-Yoshitake, Y. Okada, Y. Noda, R. Takemura, H. Yamazaki, and N. Hirokawa. 1994. KIF1B: a novel microtubule plus end-directed monomeric motor protein for mitochondria transport. *Cell.* 79:1209–1220.
- Noda, Y., Y. Sato-Yoshitake, S. Kondo, M. Nangaku, and N. Hirokawa. 1995. KIF2 is a new anterograde microtubule based motor which transport membranous organelles distinct from those carried by KHC or KIF3A/B. *J. Cell Biol.* 129:157–167.
- Okada, Y., H. Yamazaki, Y. Sekine-Aizawa, and N. Hirokawa. 1995. The neuron-specific kinesin superfamily protein KIF1A is a unique monomeric motor for anterograde axonal transport of synaptic vesicle precursors. *Cell.* 81:769–780.
- Quiroga, S., R.S. Garofalo, and K.H. Pfenninger. 1995. Insulin-like growth factor I receptors of fetal brain are enriched in nerve growth cones and contain a  $\beta$ -subunit variant. *Proc. Natl. Acad. Sci. USA.* 92:4309–4312.
- Saito, N., Y. Okada, Y. Noda, Y. Kinoshita, S. Kondo, and N. Hirokawa. 1997. KIFC2 is a novel neuron-specific C-terminal type kinesin superfamily motor for dendritic transport of multivesicular body-like organelles. *Neuron.* 18:425–438.
- Scholey, J.M., M.E. Porter, P.M. Grisson, and J.R. McIntosh. 1985. Identification of kinesin in sea urchin eggs and evidence for its localization in the mitotic spindle. *Nature (Lond.)* 318:483–486.
- Tanaka E., and J. Sabry. 1995. Making the connection: cytoskeletal rearrangements during growth cone guidance. *Cell.* 83:171–176.
- Ueda, T., P. Greengard, K. Berzina, R. Cohen, F. Blomberg, J. Grab, and P. Siekevitz. 1979. Subcellular distribution in cerebral cortex of two proteins phosphorylated by a cAMP-dependent kinase. *J. Cell Biol.* 83:308–319.
- Ullrich, A., A. Gray, A.W. Tam, T. Yang-Fen, M. Tsubokawa, C. Collins, W. Henzel, T. LeBon, S. Kathuria, E. Chen, et al., 1986. Insulin-like growth factor receptor primary structure: comparison with insulin receptor suggests structural determinants that define functional specificity. *EMBO (Eur. Mol. Biol. Organ.)* 5:2503–2512.
- Vale, R.D., B.L. Schnapp, T.S. Reese, and M.S. Sheetz. 1985. Organelle, bead, and microtubule translocation promoted by soluble factors from squid giant axons. *Cell.* 40:559–569.
- Vallee, R. 1982. A taxol-dependent procedure for the isolation of microtubules and microtubule-associated proteins (MAPs). *J. Cell Biol.* 92:435–442.
- Walczak, C.E., T. Mitchison, A. Desai. 1996. XKCM1: a *Xenopus* kinesin-related protein that regulates microtubule dynamics during mitotic spindle assembly. *Cell.* 84:37–47.
- Wagner, R. 1995. The state of the art in antisense research. *Nat. Med.* 1:1116–1118.
- Werner, H., M. Woloschak, B. Stannard, Z. Shenn-Orr, C.T. Roberts, D. LeRoith. 1991. *In Insulin-like Growth Factors: Molecular and Cellular Aspects.* D. LeRoith, editor. CRC Press, Boca Raton, FL. 17–47.
- Wordeman, L., and T. Mitchison. 1995. Identification and partial characterization of mitotic centromere-associated kinesin, a kinesin-related protein that associates with centromeres during mitosis. *J. Cell Biol.* 128:95–105.
- Yamazaki, H., T. Nakata, Y. Okada, and N. Hirokawa. 1995a. KIF3A/B: a heterodimeric kinesin superfamily protein that works as a microtubule plus end-directed motor for organelle transport. *J. Cell Biol.* 130:1387–1399.
- Yamazaki, T., D.J. Selkoe, and E.H. Koo. 1995b. Trafficking of cell surface  $\beta$ -amyloid precursor protein: retrograde and transcytotic transport in cultured neurons. *J. Cell Biol.* 129:431–442.
- Yankner, B., L. Benowitz, L. Villa-Komaroff, and R. Neve. 1990. Transfection of PC12 cells with the human GAP-43 gene: effects on neurite outgrowth and regeneration. *Mol. Brain Res.* 7:39–44.